Spatial structure and temporal evolution of a dayside poloidal ULF wave event

W. Liu,[1,2] T. E. Sarris,[2,3] X. Li,[2,4] Q.-G. Zong,[5] R. Ergun,[2] V. Angelopoulos,[6] and K. H. Glassmeier[7,8]

Received 29 August 2011; accepted 11 September 2011; published 11 October 2011.

[1] We investigate a strong poloidal ultralow frequency wave event in the noon sector observed by THEMIS and LANL satellites on 29 May 2007. From 07:00 to 10:00 UT, the five THEMIS satellites that were lined up in similar outbound orbits consecutively observed narrow-band poloidal pulsations from 10 to 4 mHz. The wave activity covered a broad region from 09:00 to 13:30 LT azimuthally and 5 to 9.5 R_E radially. The radial extent and power of the wave decreased with time from 07:00 to 08:30 UT, suggesting a decay process with a time scale of hours. In the region outside the plasmapause, the wave power was observed to decrease then increase from 08:00 to 09:00 UT with a rapid temporal variation. The decrease in wave power, which suggests fast decay (within one hour), might be related to the evolution of the plasmasphere. The subsequent increase could possibly be related to a regeneration process by a surface wave at the plasmapause. We suggest that a coupling between the surface wave and the resonance of the field line around the plasmapause takes place when the density inside the plasmapause is twice the density outside the plasmapause. **Citation:** Liu, W., T. E. Sarris, X. Li, Q.-G. Zong, R. Ergun, V. Angelopoulos, and K. H. Glassmeier (2011), Spatial structure and temporal evolution of a dayside poloidal ULF wave event, *Geophys. Res. Lett.*, *38*, L19104, doi:10.1029/2011GL049476.

1. Introduction

[2] Ultralow frequency (ULF) waves, oscillations commonly observed in the Earth's magnetosphere with frequencies from roughly 1 mHz to 1 Hz, are classified into several groups based on frequency. Their Pc4 and Pc5 bands (2 to 22 mHz) can have significant influence on energetic particles with similar drift frequency in the magnetosphere [e.g., *Elkington et al.*, 1999; *Li et al.*, 2001, 2005].

[3] After decades of ULF wave studies, many generation mechanisms for these waves have been suggested. The solar wind is believed to be the main external source, through either the Kelvin-Helmholtz instability (KHI) [*Southwood*, 1968; *Pu and Kivelson*, 1983] or variations in solar wind dynamic pressure, including periodic variations [*Kepko and Spence*, 2003] and sudden impulses [*Zong et al.*, 2007, 2009; *Zhang et al.*, 2010; *Sarris et al.*, 2010]. Waves in the same frequency band can also be generated in the foreshock region through cyclotron resonance of ions reflected at the bow shock when the angle between the interplanetary magnetic field (IMF) orientation and the Sun-Earth line (IMF cone angle) is small. Those waves can be propagated to the magnetopause, driving ULF waves in the magnetosphere [*Takahashi et al.*, 1984]. Internal sources during periods of enhanced geomagnetic activity, including drift-bounce resonance of partial ring current ions [*Southwood and Kivelson*, 1982] and bursty bulk flows during substorms [*Kepko et al.*, 2001; *Cao et al.*, 2008, 2010], have also been suggested. In general, external sources are believed to generate ULF waves in a broader region with a lower mode number, whereas internal sources are thought to generate ULF waves locally with a higher mode number.

[4] With single-spacecraft measurements, it is difficult to distinguish between spatial and temporal effects. With the benefit of small separations between the four satellites of the CLUSTER mission, investigations have been performed to separate spatial from temporal characteristics of magnetospheric poloidal waves [e.g., *Schäfer et al.*, 2007, 2008]. They found observational evidence of poloidal waves with high azimuthal wave number, as predicted theoretically by *Klimushkin et al.* [2004] and others. The THEMIS mission [*Angelopoulos*, 2008], five identical satellites (TH-A through TH-E) launched into near equatorial orbits on 17 February 2007, provides multi-point observations with larger separations. As shown by *Sarris et al.* [2009, 2010] and *Liu et al.* [2009, 2010], THEMIS satellites are ideal for studying the large-scale ULF-wave phenomena. In this paper, we present a unique ULF event observed on 29 May 2007, the spatial and temporal variations of which are distinguished using multi-point magnetic field measurements from the THEMIS FGM [*Auster et al.*, 2008] and LANL SOPA instruments.

2. Observations

[5] On 29 May 2007 the five THEMIS satellites were in coast phase (travelling in the same orbit) in the following order: TH-B, TH-D, TH-C, TH-E, TH-A, with an apogee of 14.7 R_E and a perigee of 1.1 R_E, as shown in Figure 1. In Figures 2a–2c, we plot the overviews of the wavelet power

[1]School of Astronautics, Beihang University, Beijing, China.
[2]Laboratory for Atmospheric and Space Physics, University of Colorado at Boulder, Boulder, Colorado, USA.
[3]Space Research Laboratory, Democritus University of Thrace, Xanthi, Greece.
[4]Department of Aerospace Engineering Sciences, University of Colorado at Boulder, Boulder, Colorado, USA.
[5]Institute of Space Physics and Applied Technology, Peking University, Beijing, China.
[6]Institute of Geophysics and Planetary Physics, University of California, Los Angeles, California, USA.
[7]Institute for Geophysics and Extraterrestrial Physics, Technical University of Braunschweig, Braunschweig, Germany.
[8]Max Planck Institute for Solar System Research, Katlenburg-Lindau, Germany.

0094-8276/11/2011GL049476

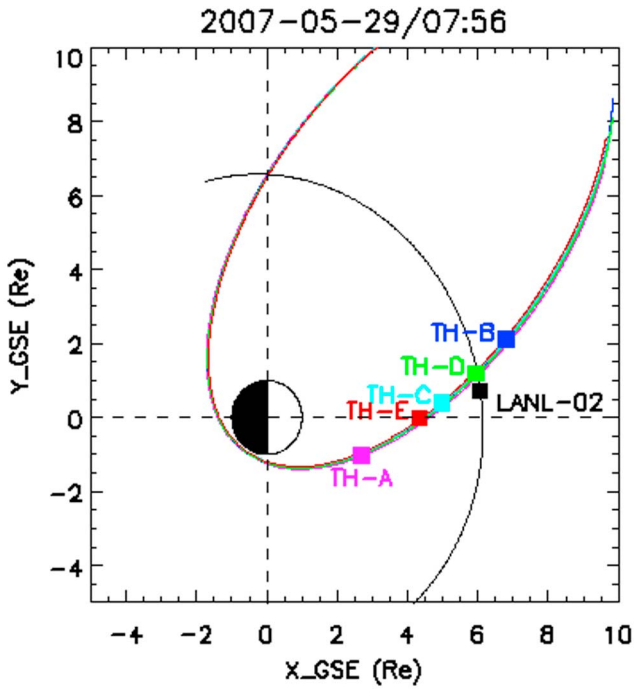

Figure 1. The X-Y view of the locations of the THEMIS and LANL-2002 satellites at 07:56 UT on 29 May 2007 in the GSE coordinate system.

spectra of the three magnetic field components in the Mean Field Aligned (MFA) coordinate system (B_r: radial, B_φ: azimuthal and $B_{//}$: parallel) observed by the leading probe TH-B (see Figures S1–S5 in the auxiliary material for all five satellites).[1] TH-B observed increases in narrow-band wave power at ~10 mHz in all three magnetic field components at 5.23 R_E around 06:40 UT, perhaps related to plasmapause crossing. After this, narrow-band wave activity is observed until ~10:00 UT. The wave power in the radial component is stronger than in the other two components (peak power of ~9 × 10^3 $(nT)^2$/mHz), suggesting that the fluctuation is poloidal. The frequency of the narrow-band fluctuation decreases from 10 to 4 mHz as TH-B moves outward. Its crossing of the magnetopause at ~12:10 UT is identified by a broad-band wave power increase in all three components.

[6] Energetic particle measurements from the SOPA instrument of LANL-02 are investigated during this event. The wavelet power spectra of the flux of 50-75 keV electron is plotted in Figure 2d (see Figure S6 in the auxiliary material for other channels). The narrow-band peaks at around 8 mHz in the spectra suggest that the particle fluxes are modulated by the magnetic field oscillations observed by the THEMIS satellites. The modulations start at 04:30 UT, weaken after 08:30 UT, and disappear around 09:00 UT, covering a wide local time range from 09:00 to 13:30 LT.

[7] The solar wind velocity, dynamic pressure, IMF components in GSE coordinates and IMF cone angle obtained from the OMNI database are shown in Figures 2e–2h. The solar wind was relatively quiet during this time. Its velocity decreased slowly from ~440 to ~410 km/s, and no large interplanetary shock was observed.

[8] This poloidal fluctuation was observed consecutively by all five THEMIS satellites in the order given above during their outbound passes. Figure 3a shows the wave power spectra of the magnetic field radial component observed by all satellites. The white, red, and green vertical lines indicate times at which the satellites cross 5 R_E, 6.6 R_E, and 9 R_E, respectively. These five spectra demonstrate many similarities, such as similar frequency characteristics and discrete increases (localized peaks) in power. These peaks do not seem to occur at the same time, suggesting that the discreteness is a spatial effect. The last panel of Figure 3a shows the low-energy (1–130 eV) proton density measured by the LANL-2002 satellite. The peaks at around 08:30 UT in this panel suggest satellite motion into the high-density plasmaspheric plasma. The blue vertical line indicates the time at which LANL-2002 crossed the THEMIS trajectories. The high-density plasma observed by LANL-2002 is within about 5 degrees (azimuthally) of the THEMIS trajectories.

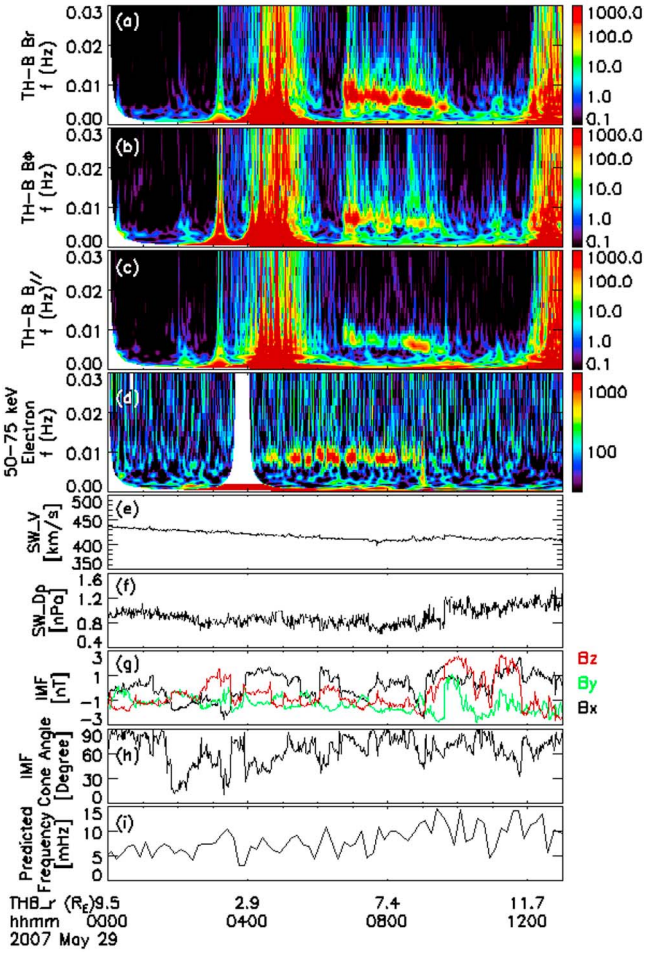

Figure 2. Wavelet power spectra of the (a) radial, (b) azimuthal and (c) parallel magnetic field components of TH-B in the MFA coordinate system and (d) LANL-2002 50–75 keV electron flux on 29 May 2007 are plotted in the top four panels, respectively. OMNI parameters, including the (e) solar wind velocity, (f) dynamic pressure, (g) IMF components in GSE, (h) IMF cone angle and (i) frequency predicted by *Takahashi et al.* [1984] are plotted in the bottom panels, respectively.

[1]Auxiliary materials are available in the HTML. doi:10.1029/2011GL049476.

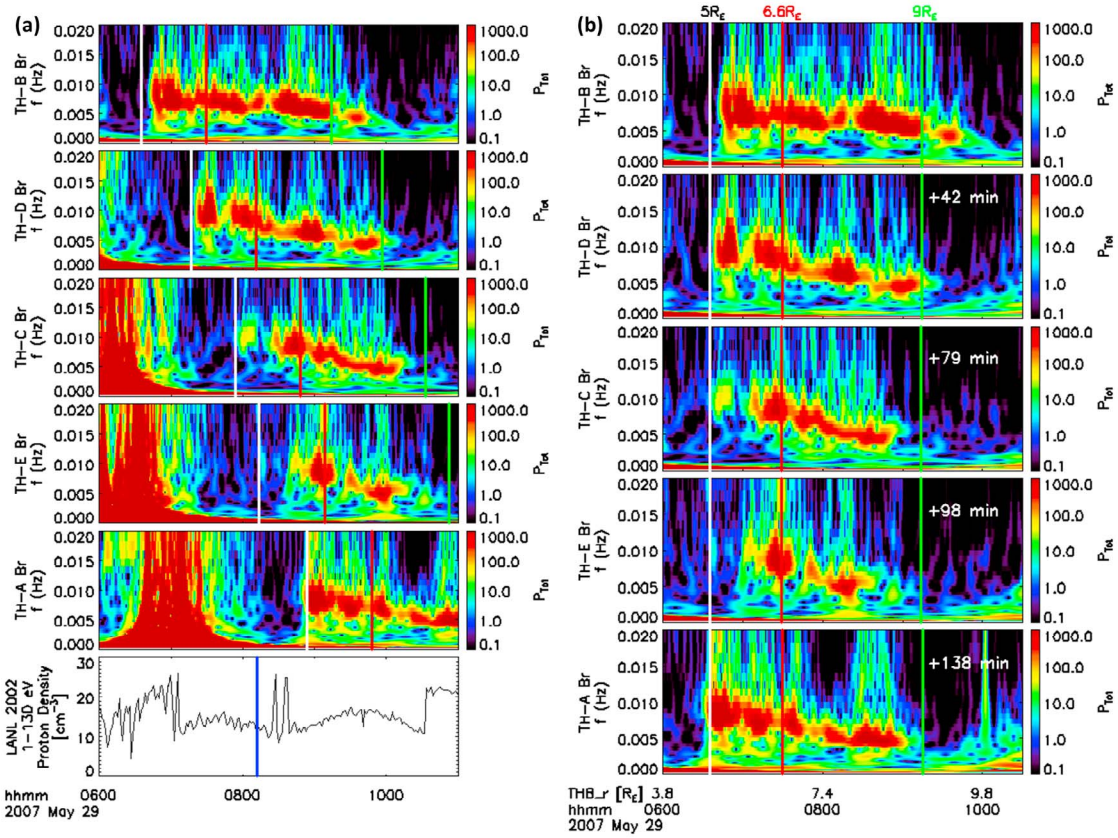

Figure 3. (a) Wave power spectra of the radial magnetic field component for five THEMIS probes on 29 May 2007 are plotted in the top five panels for TH-B, D, C, E and A, respectively; the low energy (1–130 eV) proton density and spacecraft potential of LANL-2002 are plotted in the bottom two panels, (b) Time shifted wave power spectra aligned at white lines (the time when each probe crosses 5 R_E) plotted in the same sequence as Figure 3a.

[9] In Figure 3b the wave power spectra are plotted with time shifted so as to align the satellite crossings of 5 R_E (white lines). The time shifts are 0, 42, 79, 98 and 138 minutes for probes TH-B, TH-D, TH-C, TH-E and TH-A respectively. Thus, the vertical comparison of the five panels in Figure 3b provides information on the temporal evolution of the wave power at one location. This configuration is ideal for separating temporal from spatial effects. For example, it can be observed that both the extent and the strength of the wave activity decrease with time for the first four panels, suggesting a 'slow' decay process with a time scale of hours.

[10] In the region outside 5 R_E, wave power shows temporal evolution. As seen in Figure 3b, it is stronger as

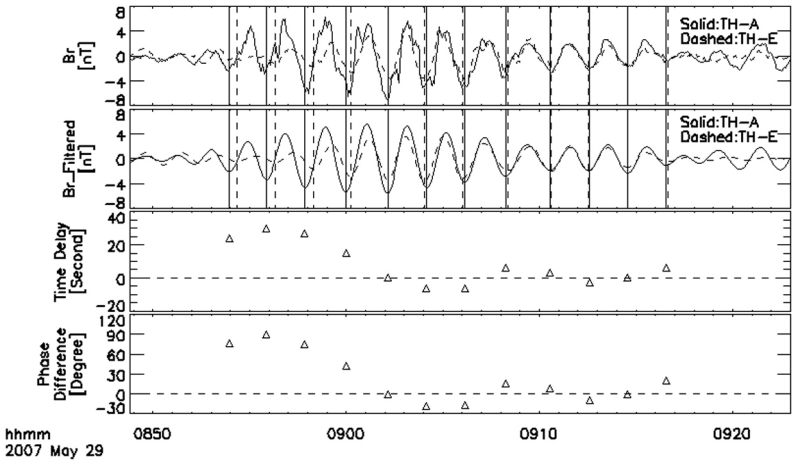

Figure 4. From top to bottom: time series of B_r of TH-A and TH-E, band-pass filtered signals of B_r of TH-A and TH-E, time delay and phase difference of the two signals around 09:00 UT, solid lines for TH-A and dashed lines for TH-E. The vertical lines in this figure indicate the negative peaks of each period identified from the band-pass filtered signals.

observed at TH-B and TH-D, weaker at TH-C, and almost disappears at TH-E, suggesting a 'fast' decay process on a time scale of less than one hour. Strong wave activity is observed again when TH-A moves into the same region about 30 minutes later, however. Comparing power spectra from TH-E and TH-A (the last two panels), we can see that within 30 minutes, the wave amplitude increases from less than 1 nT observed by TH-E to ~6 nT observed by TH-A, indicating wave regeneration in the region outside the plasmapause during this time period.

[11] To analyze this wave's generation mechanism, we plot the time series of B_r from TH-A (solid) and TH-E (dashed) at around 09:00 UT in the first panels of Figure 4. The second panel shows the band-pass filtered signals of B_r from TH-A and TH-E in the 5 to 10 mHz frequency range. The vertical lines mark the negative peaks of each period identified from those signals. The time difference between each pair of vertical lines, shown by the triangles, is calculated and plotted in the third panel. The phase difference, calculated based on the time differences and the periods, is shown in the last panel. The latter decreases from 90 to 0 degrees in the first five periods and remains at around 0 degrees for the following seven periods until the wave power decays at TH-E.

3. Discussion

[12] In this event, the passage of the five THEMIS probes through the same region (i.e., on similar orbits) with some time lag enables us to identify two decay processes with different time scales: a slower decay process, with a time-scale on the order of a couple hours, and a faster decay on the order of a few tens of minutes. Regarding the slower decay process, the observations shown in Figure 3b indicate that wave activity decays from 07:00 to 08:30 UT, with the total power in the ULF range decreasing with time as observed by the four leading probes, indicating that there is no significant energy input during this time. During this time, the outer boundary of wave activity moves inside, which might be related to the erosion of the dayside magnetosphere due to dayside reconnection under southward IMF condition, as shown in Figure 2.

[13] In addition to the slow decay of overall wave activity, there is also fast decay process in the region outside the plasmapause at around 08:30 UT as observed by TH-C and TH-E satellites (Figures 3a and 3b). Unfortunately, there is no measurement of plasmaspheric (low-energy, below several eVs) plasma density from the THEMIS satellites during this time to associate the observed waves with the density-dependent Alfvén velocity. However, as shown in Figure 3a, the LANL-2002 satellite was close to the THEMIS satellites and provided low energy proton density measurements. The two proton-density peaks between 08:20 and 08:40 UT suggest that high-density plasmaspheric plasma was coming into this region. This high-density plasma population could change the local Alfvén velocity and in turn change the local resonance frequency, leading to the rapid decay of wave activity observed by TH-E. We notice that the decaying wave power observed by TH-C and TH-E are prior to the LANL density spikes, which is probably because that THEMIS probes are ~1.5 R_E inside the geosynchronous orbit at that time.

[14] As discussed in the introduction, there are numerous mechanisms for generation of ULF waves in the inner magnetosphere. Different mechanisms excite waves in different regions [*Glassmeier and Stellmacher*, 2000]. In this event, the ULF wave activity was observed across a wide range of radial distances (5–9.5 R_E) and local time (09:00 to 13:30 LT). Electric field measurements are available from TH-C during this time, which can be used to calculate Poynting flux. The calculated Poynting flux is mainly along the field line with a small inward radial component, suggesting that it is mainly standing wave. The broad spatial coverage suggests that this poloidal event could possibly be excited by external sources; we do not have enough observations to determine the generation mechanism, however. It could be related to the time period with small IMF cone angle before 04:30 UT, as shown in Figure 1b: when the IMF cone angle is small, waves in the ULF frequency range can be generated in the foreshock region by cyclotron resonance of ions reflected at the bow shock [e.g., *Takahashi et al.*, 1984]. These waves can propagate into the magnetosheath and further generate ULF waves in the dayside magnetosphere. Based on the relation proposed by *Takahashi et al.* [1984], we estimate the frequency of waves generated by this mechanism, as plotted in the last panel of Figure 2. We find that before ~8:30 UT, the frequency is around a value of 8 mHz, which is consistent with the frequency observed by THEMIS and LANL spacecraft.

[15] A second observation that is enabled by the particular orbital configuration of THEMIS during this time, is the re-generation of ULF wave activity outside of the plasmapause around 09:00 UT: As shown in Figure 4, wave activity starts to grow at the location of TH-A at 08:54 UT, indicated by the first dashed vertical line, while TH-E observes lower wave activity with amplitudes less than 1 nT. In the first four periods, the phase difference between the two signals decreases with time. From the fifth period, the two signals oscillate with a small phase difference around 0 which remains relatively constant for the next eight periods. Several similar fine signatures can be found between the two time series during these eight periods, as shown in the first panel of Figure 4. These measurements suggest a causal relationship between the two signals. The fluctuations at TH-E are perhaps modulated by those inside at TH-A. The amplitude observed by TH-E is smaller than that of TH-A, which also argues in favour of outward propagation. Observations also suggest that this wave activity does not affect TH-C's location, about 2 R_E outward from TH-A. The characteristics of this ULF wave activity can be summarized as follows: it seems to be excited around the plasmapause, propagates outward, and is confined radially within 2 R_E.

[16] This new wave activity does not seem to be generated by external sources because the solar wind parameters do not change much from 08:30 to 09:00 UT, as shown in Figure 2. We also exclude the possibility of drift-bounce resonance because geomagnetic activity is low and there is not any particular particle population in terms of energy acting differently from other energies as suggested by THEMIS/SST data (not shown here).

[17] Based on the theoretical calculation [e.g., *Lanzerotti et al.*, 1973; *Chen and Hasegawa*, 1974], the eigen-period of a surface wave at the plasmapause is $T_s \sim \sqrt{2}l/V_{a1}$, where l is the field line length and V_{a1} is the Alfvén velocity inside the plasmapause. The field line resonance period outside the plasmapause is $T_{FLR} = 2 \int \frac{ds}{V_{az}} \sim 2l/V_{a2}$, where V_{a2} is the

Alfvén velocity outside the plasmapause. The magnetic field strength and field line length do not change sharply across the plasmapause. So if $V_{a1}/V_{a2} \sim\sqrt{2}/2$ or $n_1/n_2 = 2$, the surface wave period is close to the local field line resonance period, where n_1 and n_2 are the densities inside and outside the plasmapause. Under this condition, the surface waves can couple with the field-line resonance and can thus be amplified. We can estimate the values of n_1/n_2 of the event in this paper based on LANL low-energy proton measurements shown in the last panel of Figure 3a. The double peaks around 08:30 UT give us an estimation of n_2 of ~25/cc, whereas the background suggests n_1~12/cc, so n_1/n_2~2.1. These values satisfy the above condition. Furthermore, from the observation, the ULF wave is localized within 2 R_E radially, which is consistent with the idea that the surface wave should be damped quickly outside the plasmapause. Based on the above facts, we suggest that a surface wave could possibly be the source of the newly generated ULF wave.

[18] Surface waves can be excited at the plasmapause by an impulse which has a frequency spectrum that covers the surface wave eigenfrequency. The impulse could be attributed to external sources, disturbances in ionosphere, or, most likely in this case, motions of the plasmapause. Surface waves decay exponentially away from the plasmapause [*Lanzerotti et al.*, 1973] and their effects are thus negligible if the coupling condition is not satisfied. However, if the condition is satisfied, which is possible only in the region outside the plasmapause, the field lines are disturbed in the normal direction of the plasmapause. Thus, if the normal direction of the plasmapause is close to the radial direction, then mostly poloidal waves are expected to be generated, whereas toroidal waves could be generated in cases where the plasmapause is more perturbed.

4. Conclusions

[19] A poloidal ULF wave event with broad spatial coverage is observed by THEMIS and LANL spacecraft. The configuration of THEMIS probes enables us to investigate temporal and spatial effects in this event. We demonstrate the impact of the plasmapause on ULF waves. The evolution of the plasmasphere could lead to a fast decay of wave power outside the plasmapause. We also demonstrate that it is possible that surface waves can generate poloidal waves in the region outside the plasmapause, as the resonant condition is met in this case. The newly generated waves have a relatively large amplitude (6 nT in this event), and thus have a potential impact on radiation particle transport and acceleration.

[20] **Acknowledgments.** This work is supported by NSFC grant (41104109), NASA grants (NNX10AQ48G and NAS5-02099), NSF grant (ATM 0842388), other grants from the NSFC (40621003, 40728005 and 40931054) and the 973 program of China (2011CB811404). The work by WL was also supported by the fund for outstanding overseas researcher from the Beihang University (YWF-11-03-H-020). The work by TES was also supported by ΔΠΘ ETAA-1927. The work by KHG was supported by the German Zentrum für Luft- und Raumfahrt under grant 50QP0402. We acknowledge the OMNI group at NASA/GSFC and LANL for making solar wind parameters and LANL data available. We also thank Judy Hohl for her valuable suggestions on improving the paper.

[21] The Editor thanks Larry Kepko for his assistance in evaluating this paper.

References

Angelopoulos, V. (2008), The THEMIS Mission, *Space Sci. Rev.*, *141*, 453–476, doi:10.1007/s11214-008-9378-4.

Auster, H. U., et al. (2008), The THEMIS fluxgate magnetometer, *Space Sci. Rev.*, *141*, 235–264, doi:10.1007/s11214-008-9365-9.

Cao, J.-B., et al. (2008), Characteristics of middle- to low-latitude Pi2 excited by bursty bulk flows, *J. Geophys. Res.*, *113*, A07S15, doi:10.1029/2007JA012629.

Cao, J.-B., et al. (2010), Geomagnetic signatures of current wedge produced by fast flows in a plasma sheet, *J. Geophys. Res.*, *115*, A08205, doi:10.1029/2009JA014891.

Chen, L., and A. Hasegawa (1974), A theory of long-period magnetic pulsations: 2. Impulse excitation of surface eigenmode, *J. Geophys. Res.*, *79*(7), 1033–1037, doi:10.1029/JA079i007p01033.

Elkington, S. R., M. K. Hudson, and A. A. Chan (1999), Acceleration of relativistic electron via drift-resonant interaction with toroidal-mode Pc-5 ULF oscillations, *Geophys. Res. Lett.*, *26*, 3273–3276, doi:10.1029/1999GL003659.

Glassmeier, K.-H., and M. Stellmacher (2000), Concerning the local time asymmetry of Pc5 wave power at the ground and field line resonance widths, *J. Geophys. Res.*, *105*, 18,847–18,855, doi:10.1029/2000JA900037.

Kepko, L., and H. E. Spence (2003), Observations of discrete, global magnetospheric oscillations directly driven by solar wind density variations, *J. Geophys. Res.*, *108*(A6), 1257, doi:10.1029/2002JA009676.

Kepko, L., et al. (2001), Flow bursts, braking, and Pi2 pulsations, *J. Geophys. Res.*, *106*(A2), 1903–1915, doi:10.1029/2000JA000158.

Klimushkin, D., et al. (2004), Toroidal and poloidal Alfvén waves with arbitrary azimuthal wavenumbers in a finite pressure plasma in the Earth's magnetosphere, *Ann. Geophys.*, *22*, 267–287, doi:10.5194/angeo-22-267-2004.

Lanzerotti, L. J., et al. (1973), Excitation of the plasmapause at ultralow frequencies, *Phys. Rev. Lett.*, *31*(10), 624–628, doi:10.1103/PhysRevLett.31.624.

Li, X., M. Temerin, D. N. Baker, G. D. Reeves, and D. Larson (2001), Quantitative prediction of radiation belt electrons at geostationary orbit based on solar wind measurements, *Geophys. Res. Lett.*, *28*, 1887, doi:10.1029/2000GL012681.

Li, L., J. Cao, and G. Zhou (2005), Combined acceleration of electrons by whistler-mode and compressional ULF turbulences near the geosynchronous orbit, *J. Geophys. Res.*, *110*, A03203, doi:10.1029/2004JA010628.

Liu, W., T. E. Sarris, X. Li, S. R. Elkington, R. Ergun, V. Angelopoulos, J. Bonnell, and K. H. Glassmeier (2009), Electric and magnetic field observations of Pc4 and Pc5 pulsations in the inner magnetosphere: A statistical study, *J. Geophys. Res.*, *114*, A12206, doi:10.1029/2009JA014243.

Liu, W., T. E. Sarris, X. Li, R. Ergun, V. Angelopoulos, J. Bonnell, and K. H. Glassmeier (2010), Solar wind influence on Pc4 and Pc5 ULF wave activity in the inner magnetosphere, *J. Geophys. Res.*, *115*, A12201, doi:10.1029/2010JA015299.

Pu, Z. Y., and M. G. Kivelson (1983), Kelvin-Helmholtz instability at the magnetopause: Solution for compressible plasmas, *J. Geophys. Res.*, *88*, 841–852, doi:10.1029/JA088iA02p00841.

Sarris, T. E., et al. (2009), Characterization of ULF pulsations by THEMIS, *Geophys. Res. Lett.*, *36*, L04104, doi:10.1029/2008GL036732.

Sarris, T. E., W. Liu, X. Li, K. Kabin, E. R. Talaat, R. Rankin, V. Angelopoulos, J. Bonnell, and K.-H. Glassmeier (2010), THEMIS observations of the spatial extent and pressure-pulse excitation of field line resonances, *Geophys. Res. Lett.*, *37*, L15104, doi:10.1029/2010GL044125.

Schäfer, S., et al. (2007), Spatial and temporal characteristics of poloidal waves in the terrestrial plasmasphere: A CLUSTER case study, *Ann. Geophys.*, *25*, 1011–1024, doi:10.5194/angeo-25-1011-2007.

Schäfer, S., et al. (2008), Spatio-temporal structure of a poloidal Alfvén wave detected by Cluster adjacent to the dayside plasmapause, *Ann. Geophys.*, *26*, 1805–1817, doi:10.5194/angeo-26-1805-2008.

Southwood, D. J. (1968), The hydromagnetic stability of the magnetopause boundary, *Planet. Space Sci.*, *16*, 587–605, doi:10.1016/0032-0633(68)90100-1.

Southwood, D. J., and M. G. Kivelson (1982), Charged particle behavior in low-frequency geomagnetic pulsations. II. Graphical approach, *J. Geophys. Res.*, *87*, 1707–1710, doi:10.1029/JA087iA03p01707.

Takahashi, K., R. L. McPherron, and T. Terasawa (1984), Dependence of the spectrum of Pc 3-4 pulsations on the interplanetary magnetic field, *J. Geophys. Res.*, *89*(A5), 2770–2780, doi:10.1029/JA089iA05p02770.

Zhang, X. Y., Q.-G. Zong, Y. F. Wang, H. Zhang, L. Xie, S. Y. Fu, C. J. Yuan, C. Yue, B. Yang, and Z. Y. Pu (2010), ULF waves excited by negative/positive solar wind dynamic pressure impulses at geosynchronous orbit, *J. Geophys. Res.*, *115*, A10221, doi:10.1029/2009JA015016.

Zong, Q.-G., et al. (2007), Ultralow frequency modulation of energetic particles in the dayside magnetosphere, *Geophys. Res. Lett.*, *34*, L12105, doi:10.1029/2007GL029915.

Zong, Q.-G., X.-Z. Zhou, Y. F. Wang, X. Li, P. Song, D. N. Baker, T. A. Fritz, P. W. Daly, M. Dunlop, and A. Pedersen (2009), Energetic electron response to ULF waves induced by interplanetary shocks in the outer radiation belt, *J. Geophys. Res.*, *114*, A10204, doi:10.1029/2009JA014393.

V. Angelopoulos, Institute of Geophysics and Planetary Physics, University of California, 3845 Slichter Hall, Los Angeles, CA 90095, USA.

R. Ergun and X. Li, Laboratory for Atmospheric and Space Physics, University of Colorado at Boulder, 1234 Innovation Dr., Boulder, CO 80303, USA.

K. H. Glassmeier, Institute for Geophysics and Extraterrestrial Physics, Technical University of Braunschweig, Mendelssohnstr. 3, D-38106 Braunschweig, Germany.

W. Liu, School of Astronautics, Beihang University, Beijing 100191, China. (liuwenlong@buaa.edu.cn)

T. E. Sarris, Space Research Laboratory, Democritus University of Thrace, Vasilisis Sofias 1, GR-67100 Xanthi, Greece.

Q.-G. Zong, Institute of Space Physics and Applied Technology, Peking University, Beijing 100871, China.